

ON CEPHEID DISTANCE SCALE BIAS DUE TO STELLAR COMPANIONS AND CLUSTER POPULATIONS

RICHARD I. ANDERSON^{1,2} AND ADAM G. RIESS^{2,3}

¹*European Southern Observatory, Karl-Schwarzschild-Str. 2, D-85748 Garching b. München, Germany*

²*Department of Physics and Astronomy, The Johns Hopkins University, 3400 N Charles St, Baltimore, MD 21218, USA*

³*Space Telescope Science Institute, 3700 San Martin Dr, Baltimore, MD 21218, USA*

(Received June 20, 2022; Revised; Accepted)

ABSTRACT

State-of-the art photometric measurements of extragalactic Cepheids account for the mean additional light due to chance superposition of Cepheids on crowded backgrounds through the use of artificial star measurements. However, light from stars physically associated with Cepheids may bias relative distance measurements if the changing spatial resolution along the distance ladder significantly alters the amount of associated blending. We have identified two regimes where this phenomenon may occur: Cepheids in wide binaries and open clusters.

We estimate stellar association bias using the photometric passbands and reddening-free Wesenheit magnitudes used to set up the Riess et al. (2016) distance scale. For wide binaries, we rely on Geneva stellar evolution models in conjunction with detailed statistics on intermediate-mass binary stars. For the impact of cluster stars, we have compiled information on the frequency of Cepheids occurring in clusters and measured the typical cluster contribution in M31 via deep *HST* imaging provided by the PHAT project.

We find that the dominant effect on the distance scale comes from Cepheids in clusters, despite cluster Cepheids being a relatively rare phenomenon. Wide binaries have a negligible effect on H_0 that is on the order of 0.004% for long-period Cepheids observed in the near-infrared or when considering Wesenheit magnitudes. We estimate that blending due to cluster populations has previously resulted in an overestimate of H_0 by approximately 0.2%. Correcting for this bias, we obtain $H_0 = 73.06 \pm 1.76 \text{ km s}^{-1} \text{ Mpc}^{-1}$, which remains in 3.3σ tension with the *Planck* value. We conclude that stellar association bias does not constitute a limit for measuring H_0 with an accuracy of 1%.

Keywords: Cepheids — cosmology — distance scale

arXiv:1712.01065v1 [astro-ph.SR] 4 Dec 2017

1. INTRODUCTION

The extragalactic distance scale provides a crucial measure of the present-day expansion rate of the universe, i.e. the Hubble constant H_0 . Historically, there has been great interest in measuring H_0 with ever improving accuracy (for recent reviews, cf. [Freedman & Madore 2010](#); [Livio & Riess 2013](#)). A significant improvement was the *Hubble Key Project* ([Freedman et al. 2001](#)), which reached the 10% accuracy level. Since then, improved observing strategies that favor data homogeneity, better error analysis and propagation, larger samples of Cepheids in SN-host galaxies ([Riess et al. 2011](#), henceforth: R+11), and better trigonometric parallaxes of Cepheids in the Milky Way have enabled considerable improvements, so that the current accuracy of H_0 now figures at 2.4% ($73.24 \pm 1.74 \text{ km s}^{-1} \text{ Mpc}^{-1}$, cf. [Riess et al. 2016](#), henceforth: R+16). In the R+16 implementation, classical Cepheids provide a geometric calibration for type-Ia supernovae peak luminosities and covariance is taken into account by modeling the distance scale globally. A distance-scale independent estimate of H_0 with 3.8% precision ($72.8 \pm 2.4 \text{ km s}^{-1} \text{ Mpc}^{-1}$) has been obtained using time delays observed in gravitationally lensed quasars using a prior on Ω_M ([Bonvin et al. 2017](#)), which is in good agreement with R+16. Exchanging SNIa optical magnitudes with near-IR data also yields a result consistent with this value of H_0 ([Dhawan et al. 2017](#), $72.8 \pm 1.6 \pm 2.7 \text{ km s}^{-1} \text{ Mpc}^{-1}$). Finally, gravitational wave events may provide single digit accuracy on H_0 in the future ([Del Pozzo 2012](#); [Abbott et al. 2017](#)). Of course, many complementary efforts are under way to accurately measure H_0 , e.g. using standard candles belonging to older stellar populations (e.g. [Beaton et al. 2016](#)).

There are two key motivations for continuing to push H_0 accuracy. First, H_0 can serve as a powerful prior for analyses of the Cosmic Microwave Background (CMB) and knowing H_0 to 1% accuracy would significantly improve the uncertainties on the dark energy equation of state σ_w ([Suyu et al. 2012](#); [Weinberg et al. 2013](#); [Manzotti et al. 2016](#)), which is crucial for understanding the origin and nature of the universe’s accelerated expansion ([Riess et al. 1998](#); [Perlmutter et al. 1999](#)).

Second, R+16 have shown that H_0 measured directly using a state-of-the-art distance scale now differs by 3.4σ from the value inferred from the *Planck* satellite’s measurements of the CMB assuming Λ CDM ([Planck Collaboration et al. 2016](#)). This has since been confirmed independently ([Cardona et al. 2017](#); [Follin & Knox 2017](#)). Moreover, this difference cannot be explained solely by invoking systematic errors in the *Planck* data ([Addison et al. 2017](#)). If this difference is amplified by even more

accurate determinations of H_0 , then such a discrepancy could lead to the exciting conclusion that the presently-accepted cosmological model is incomplete.

Of course, detailed investigations of systematics intervening in H_0 measurements are required before new physics may be credibly invoked to explain this observed difference. Large efforts are already underway to this end, focusing on all aspects of the distance ladder. For Cepheids specifically, possible non-linearities or metallicity-dependence of the Leavitt Law, i.e., the Period-luminosity Relation of Cepheids ([Leavitt & Pickering 1912](#), PLR), have received much recent attention (e.g. [Sandage et al. 2004](#); [Sakai et al. 2004](#); [Storm et al. 2004](#); [Ngeow & Kanbur 2006](#); [García-Varela et al. 2013](#); [Inno et al. 2013](#); [Kodric et al. 2015](#); [Bhardwaj et al. 2016](#); [Wielgórski et al. 2017](#)). Yet, none of these effects have been confirmed to significantly impact H_0 .

The crucial geometric footing for the cosmic distance scale is currently being rebuilt thanks to technical advances in accurately measuring trigonometric parallaxes of classical Cepheids. Specifically, observations made in spatial scanning mode using *HST/WFC3* ([Riess et al. 2014](#); [Casertano et al. 2016](#), [Riess et al. in prep.](#)) are used to measure parallax of a number of Galactic Cepheids with $30 - 40 \mu\text{arcsec}$ accuracy (cf. also [Anderson et al. 2016b](#)). On an even larger scale, the ESA mission *Gaia* is currently measuring parallax of approximately 300 Galactic Cepheids with better than 3% accuracy ([Gaia Collaboration et al. 2016b,a, 2017a](#)). Thus, the Galactic calibration of the Leavitt law will be considerably improved compared to the previous calibration based on 10 Cepheids with parallaxes known to better than 10% accuracy ([Benedict et al. 2007](#)).

The spatial coincidence of multiple light sources within a detector resolution element or PSF (henceforth: *blending*) becomes increasingly likely with distance, since the physical scale (in pc) of a single pixel increases with distance for a fixed plate scales (in arcsec per pixel). Thus, apparent Cepheid magnitudes are expected to be increasingly affected by “parasitic” flux contributions the farther away the galaxy in which they reside.

Blending can occur due to chance superposition (e.g. field stars in a distant galaxy of interest) or physical association (e.g. companion stars in binaries or cluster member stars). Notably, blending due to chance superposition can be effectively corrected using local, artificial star tests (R+11) that estimate the average light contribution per pixel due to field stars near the object of interest. However, stars physically associated with Cepheids are necessarily close (within a few parsecs) and thus potentially unresolved, and the properties of their

Definitions		
$M_{\text{MW}}(P)$	$= m_{\text{Cep,MW}} - \mu_{0,\text{Gaia}}$	$= -2.5 \cdot \log(\mathcal{F}_{\text{Cep}}(P) + \mathcal{F}_{\text{Comp,near}}) - 5 \log d_{\text{Cep}} + 5$
$M_{\text{LMC}}(P)$	$= m_{\text{Cep,LMC}} - \mu_{0,\text{LMC}}$	$= -2.5 \cdot \log(\mathcal{F}_{\text{Cep}}(P) + \mathcal{F}_{\text{Comp,near}} + \mathcal{F}_{\text{Comp,wide}}) - 5 \log d_{\text{LMC}} + 5$
$M_{\text{SN}}(P)$	$= m_{\text{Cep,SN}} - \mu_{0,\text{Gaia}}$	$= -2.5 \cdot \log(\mathcal{F}_{\text{Cep}}(P) + \mathcal{F}_{\text{Comp,near}} + \mathcal{F}_{\text{Comp,wide}} + \mathcal{F}_{\text{Clusters}}) -$ $-m_{\text{Cep,MW}} + M_{\text{MW}}(P)$
ΔM_{SN}	$= M_{\text{SN}} - M_{\text{MW}}$	$= f_{\text{wb}} \cdot \Delta M_{\text{wb}} + f_{\text{CC}} \cdot \Delta M_{\text{Cl}}$
f_{wb}		fraction of Cepheids with wide ($400 \lesssim a_{\text{rel}} \lesssim 4000$ AU) companions, cf. §2.1
ΔM_{wb}		typical brightening by a companion on a wide orbit, cf. §2.2
f_{CC}		fraction of Cepheids occurring in clusters, cf. §3.1
ΔM_{Cl}		typical brightening due to cluster stars. cf. §3.2

Table 1. Definition of stellar association bias. d denotes distance, \mathcal{F} flux received, m apparent magnitude, M absolute magnitude, μ distance modulus, and P pulsation period. Subscript SN refers to a typical SN-host galaxy, e.g. in the *SHOES* project (R+16). M_{SN} is assumed to be computed using a Galactic PLR calibrated using *Gaia* parallaxes of Milky Way (MW) Cepheids.

light contribution may differ from that of the (possibly crowded) field stars. Given a fixed plate scale, the ability to resolve physically associated stars depends on distance, so that flux contributed by physically associated stars cannot always be estimated directly from the observations of each galaxy. Although it would be possible to apply a homogeneous aperture of fixed physical scale to all galaxies (including the MW), this would a) add considerable noise (in particular in the MW) and b) lack the external view of MW Cepheids analogous to their extragalactic counterparts. Table 1 provides an overview of the physically associated objects blending into a Cepheid’s PSF on different “rungs” of the distance ladder.

Previous studies have targeted blending effects due to chance superposition by estimating the brightening of Cepheids as a function of angular resolution by comparing apparent magnitudes measured using observations from the ground and from Space (Stanek & Udalski 1999; Mochejska et al. 2000, 2001; Bresolin et al. 2005; Vilardell et al. 2007; Senchyna et al. 2015). The claim that blending causes significant distance scale bias presented in some of these studies requires revision for several reasons. First, blending by field stars is routinely corrected using artificial star tests. Second, the distinction between physically associated objects, such as cluster members and companion stars, and nearby field stars had previously remained somewhat unclear. This distinction is crucial, however, and can be made much more clearly now thanks to updated statistics on stellar multiplicity—in particular regarding wide companions—and cluster membership of Cepheids, as well as deep *HST* imaging of a significant portion of M31. Notably, the common assertion that Cepheids frequently occur in star clusters has remained largely

$\Delta\mathcal{F}$	m	M	$\mu = m - M$	$d = 10^{0.2(\mu+5)}$	$H_0 = v/d$
↑	↓	=	↓ (closer)	↓ (closer)	↑ (faster)

Table 2. Visualizing the impact of added flux contributions to Cepheids in SN Ia hosts due to wide companion stars or cluster members on H_0 , in case the Leavitt law is calibrated using Cepheids that are not subject to such contamination.

unchecked and has led to the erroneous (cf. Sec. 3.1) interpretation that previous blending estimates were primarily sensitive to physically associated objects instead of chance alignment. Finally, the discussion of blending-related issues has not yet been updated to reflect the current state-of-the-art calibration of the distance scale, which utilizes artificial star corrections, or the typical photometric passbands used to measure H_0 . Thus, this *article* seeks to clarify the impact of physically associated stars on the distance scale.

To this end, we estimate the photometric bias due to blending of physically associated objects and its influence on the H_0 measurement presented in R+16. The bias exists because some physically associated objects (wide binaries and cluster stars) are spatially resolved on Galactic scales, whereas they cannot be identified or de-biased in distant galaxies that set the luminosity zero-point for type-Ia supernovae. Thus, stellar association bias leads to systematic differences between Leavitt laws observed along the distance ladder. Table 2 illustrates the direction of this bias for different quantities of interest.

We estimate separately the bias contribution due to companion and cluster stars. §2 details the estimation of bias due to companion stars on wide orbits ($a_{\text{rel}} > 400$ au) using binary statistics and state-of-the-art stel-

lar evolution models. We adopt a synthetic approach for wide binaries, since photometric *HST* observations of Galactic Cepheids are scant, whereas binary statistics of intermediate-mass stars have been studied in detail. Moreover, most *visual* companions to Cepheids are likely not physically associated (Evans et al. 2016b,a). §3 presents our empirical estimation of bias due to cluster stars. To this end, we review the occurrence rate of Cepheids in clusters in the Galaxy (MW), Large Magellanic Cloud (LMC), Small Magellanic Cloud (SMC), and the Andromeda galaxy (M31), and employ deep *HST* imaging of M31 by the *PHAT* project (Dalcanton et al. 2012) to obtain an empirical estimate of the average light contribution from Cepheid host cluster populations. §4 discusses relevant uncertainties and limitations of this work and provides recommendations for mitigating stellar association bias. §5 summarizes our results.

2. BINARY STARS

Cepheids frequently occur in binary or higher order multiple systems (e.g. Szabados 2003; Neilson et al. 2015), and despite long-standing efforts to detect companions even well-studied cases such as the prototype δ Cephei occasionally hold surprises (Anderson et al. 2015). Most companions of Galactic Cepheids are not spatially resolved, although several companions have been directly detected using long baseline optical interferometry (Gallenne et al. 2015). Conversely, most *visual* companions—i.e., spatially resolved stars located near a Cepheids—appear to be not physically associated, since physically bound companions seem to be limited to relative semimajor axes $a_{\text{rel}} \lesssim 4000$ au (Evans et al. 2016b,a).

Companions of high-interest long-period Galactic Cepheids (typical distance ~ 2.5 kpc, cf. Riess et al. 2014; Casertano et al. 2016) on orbits with relative semimajor axes $a_{\text{rel}} \gtrsim 400$ AU can be resolved using *HST/WFC3*'s UVIS channel ($0.04''/\text{pixel}$, i.e., separations $\gtrsim 0.1''$ are resolved). Thus, the range of companion semimajor axes contributing this bias is $400 \lesssim a_{\text{rel}} \lesssim 4000$ AU. The threshold for resolving the widest LMC companions would be $a_{\text{rel}} \gtrsim 10000$ AU.

We estimate the bias due to wide binaries using published multiplicity statistics of intermediate-mass stars in conjunction with predictions from state-of-the-art stellar evolution models. We expect this to be small since a) wide binaries are rare and b) Cepheids outshine typical companions by several magnitudes (e.g. Anderson et al. 2016b). We rely on a general compilation of intermediate-mass ($5 - 9 M_{\odot}$ Anderson et al. 2014, 2016a) star multiplicity statistics (Moe & Di Stefano 2016) rather than on Cepheid-specific multiplicity in-

formation, since the range of possible orbital semimajor axes—in particular the very wide orbits—has been more completely explored for B-stars than for the generally distant and evolved (luminous) Cepheids, which tend to outshine their companions by several magnitudes (Anderson et al. 2016b). We further base the estimate of the typical wide companion flux on stellar model predictions, since empirical estimates of this kind are not presently available.

We first discuss the occurrence rate of wide companions, f_{wb} , in §2.1, and then estimate the average flux contribution of a typical companion star, \hat{M}_{P_p} , in §2.2 to assess the possible impact on H_0 .

2.1. Wide binary fraction

We adopt $f_{\text{wb}} = 0.15$ as the fraction of MW Cepheids that have wide ($a_{\text{rel}} > 400$ au), spatially resolved, companions. This value is based on a recent comprehensive compilation of information on binary statistics that employed results from spectroscopy, eclipses, long-baseline interferometry, sparse aperture masking, adaptive optics, lucky imaging, and common proper motion (Moe & Di Stefano 2016). The de-biased multiplicity fraction of intermediate-mass stars with mass ratios $q = \mathcal{M}_2/\mathcal{M}_1 > 0.1$ in the orbital period range $\log(P_o [\text{d}]) \in [6.5, 7.5]$ is $f_{\log P_o=[6.5,7.5];q>0.1} = 0.11 \pm 0.03$. We adopt a slightly higher $f_{\text{wb}} = 0.15$ to account for a larger orbital period range of interest, i.e., $\log(P_o [\text{d}]) \in [7.0, 8.5]$, for typical Cepheid companions with $a_{\text{rel}} \in [400, 4000]$ AU and $\mathcal{M}_1 \in [5, 9] M_{\odot}$. Note that the adopted binary fraction is an upper limit in the sense that $f_{\log P_o=[6.5,7.5];q>0.1}$ also contains mass ratios $q = \mathcal{M}_{\text{Companion}}/\mathcal{M}_{\text{Cep}} \in [0.1, 0.3]$ rather than the presently adopted $q > 0.3$. This limitation is related to a) the limited mass range in the stellar isochrones and b) differences in the mass function for lower q (Moe & Di Stefano 2016). We note that detailed multiplicity statistics of late-type dwarf stars yield a very similar result for wide binaries: $f_{\text{wb,solar}} = 0.16 \cdot (1.3 \pm 0.2)$ (Halbwachs et al. 2017).

2.2. Typical companion bias based on stellar models

We estimate the light contribution by companions on wide orbits using stellar isochrones and random companion mass ratios, since the mass ratio distribution of very wide companions ($a_{\text{rel}} \approx 200 - 5000$ AU) is nearly consistent with random pairing following the initial mass function across the mass ratios of interest (Moe & Di Stefano 2016). We adopt a power law distributions, $p_q \propto q^{\gamma}$, where $\gamma = -2$ for $q > 0.3$ for stars in the mass range $5 - 9 M_{\odot}$. We draw 100,000 random mass ratios using a power law normalized such that there is a 100%

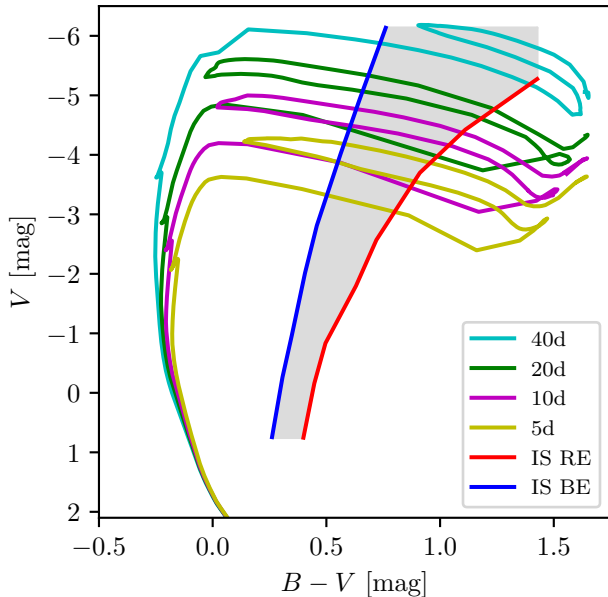


Figure 1. Solar metallicity Geneva isochrones with average initial rotation rate $\Omega/\Omega_c = 0.5$ corresponding to different pulsation periods near the blue instability strip edge during the second crossing. The instability strip shown is based on the same models (Anderson et al. 2016a).

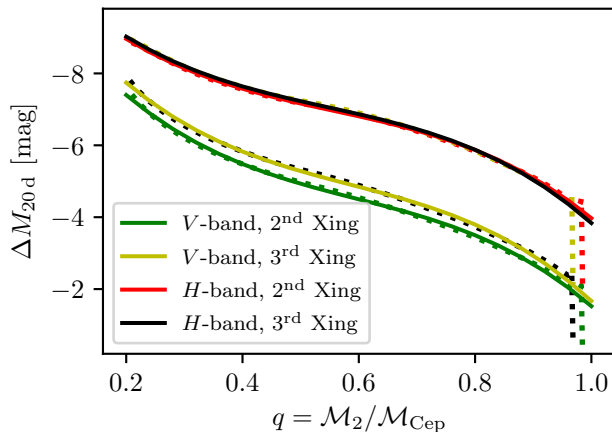


Figure 2. Contrast between a 20 d Cepheid and its Main Sequence companion as a function of mass ratio q . The corresponding isochrone is shown in Fig. 1.

chance of having a companion within $q = [0.3, 1.0]$, i.e., $\int_{0.3}^{1.0} \text{const} \cdot q'^{-2} dq' = 1$.

We estimate the typical flux contribution due to a wide binary companion as follows. Predictions of stellar properties are provided by Geneva isochrones (Ekström et al. 2012; Georgy et al. 2013; Anderson et al. 2014) of Solar metallicity ($Z = 0.014$) computed using a typical initial (ZAMS) angular rotation rate $\omega = \Omega/\Omega_{\text{crit}} = 0.5$.

For simplicity we assume that Cepheids are located near the hot edge of the instability strip (IS) determined

for these models (Anderson et al. 2016a). Although real Cepheids are distributed across the IS, this simplifying assumption eliminates the uncertainty related to the location of the cool IS edge and provides a more conservative upper limit on the companion bias, which tends to decrease for redder stars, in particular when dealing with reddening-free Wesenheit magnitudes. The blue edge of the IS was approximated by a linear fit: $\log(T_{\text{eff, BE}} [\text{K}]) = 3.9300 - 0.0447 \log L/L_{\odot}$.

The isochrones used for this estimation have been computed using a freely accessible online interpolation tool¹. The adopted isochrone ages were computed using period-age relations determined for the same models (Anderson et al. 2016a) and correspond to a range of pulsation periods of interest ($P_p = [40, 20, 10, 5]$ d). Age differences between second and third IS crossings are accounted for, i.e., a 40 d Cepheid on the second crossing is slightly younger than a 40 d Cepheid on the third crossing. Thus, the adopted isochrone ages are $\log(t [\text{yr}]) = 7.36, 7.57, 7.78,$ and 7.99 for Cepheids on second crossings, and $\log(t [\text{yr}]) = 7.41, 7.62, 7.83,$ 8.04 for third crossing Cepheids. The isochrone files list VEGA magnitudes for UBVRI (Johnson-Cousins photometric system) and JHK (Bessel) filters (Anderson et al. 2016b). Detailed comparisons with Cepheid properties have shown excellent agreement for a host of different observables (Anderson et al. 2016a).

All companion stars considered here are assumed to be main sequence stars. This implies a practical upper limit on the mass fraction $q = \mathcal{M}_2/\mathcal{M}_1 \lesssim 0.97$. Although five eclipsing LMC binary systems composed of Cepheid and red giant stars have been identified by the *Araucaria* project (e.g. Gieren et al. 2014), the short lifetime of the Cepheid evolutionary stage ($10^4 - 10^6$ yr depending on mass ($9 - 5 \mathcal{M}_{\odot}$), cf. Tab. 4 in Anderson et al. 2014) in practice limits observed pairs of evolved binary components to the shortest period Cepheids. To wit, the longest period Cepheid in such a system has $P_p = 3.8$ d (Pietrzyński et al. 2010). However, such short periods are not usually observable in distant SN host galaxies and are not relevant to the present discussion. Similarly, we do not consider white dwarf or other stellar remnant companions, although it is known that the companions of approximately $30 \pm 10\%$ of single-lined spectroscopic binaries among O and B-type stars are stellar remnants, the majority of which are white dwarfs (Wolff 1978; Garmany et al. 1980; Moe & Di Stefano 2016). Neglecting the occurrence of white dwarf companions overestimates the binary bias, since white dwarf

¹ <https://obswww.unige.ch/Recherche/evoldb/index/>

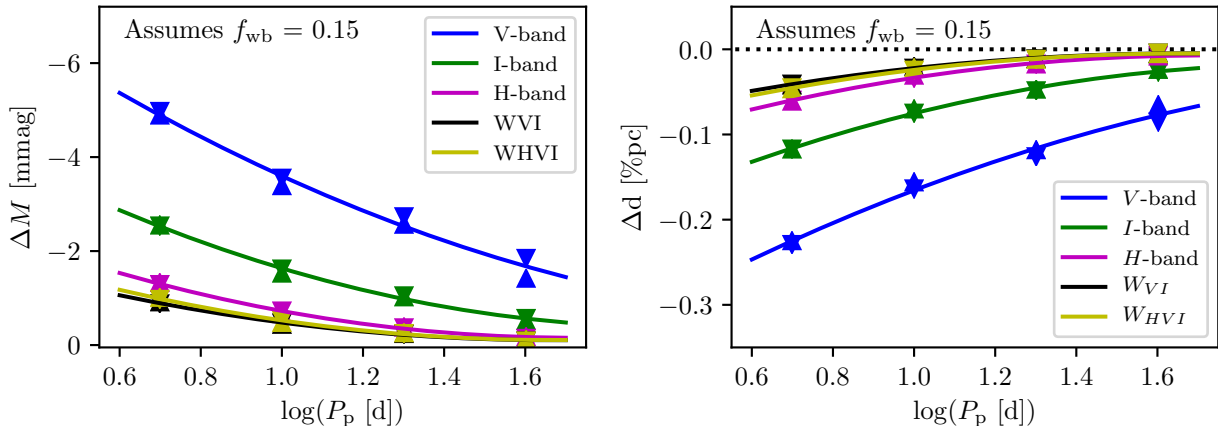


Figure 3. Estimation of bias due to wide binaries in apparent magnitude (left) and percent of distance (right). Negative ΔM indicates an apparent brightening due to additional companion flux, negative distance indicates that extragalactic distances have been underestimated by the stated amount. Both panels assume that $f_{wb} = 15\%$ of Cepheids have companions that are resolved only on Galactic, but not on extragalactic scales.

companions do not measurably affect Cepheid magnitudes, and more than compensates for neglecting the rare cases of binary systems containing a Cepheid and another evolved star. However, we here do not reduce f_{wb} to account for white dwarf companions due to a lack of detail in binary statistics. For instance, the fraction of white dwarf companions in very wide (isolated) binaries may be significantly different from single-lined spectroscopic binaries (SB1), which are more likely to undergo binary interactions. Any such correction will linearly affect the total estimated bias and can be straightforwardly applied by modifying f_{wb} according to the fraction of companions assumed to be stellar remnants.

For a fixed mass ratio, the luminosity contrast ΔM between a Cepheid and its main sequence companion depends exclusively on the Cepheid’s pulsation period P_p and IS crossing, since initial rotation rate ω and metallicity Z are assumed to be identical, and the Cepheid’s temperature is fixed to coincide with the blue IS edge.

For each isochrone, we compute magnitude differences between the Cepheid and a range of companion masses with $0.3 < q < 0.95$ based on a cubic polynomial fit in the q vs. ΔM plane. This fit yields $\Delta M(\log t; q) = \Delta M(P_p; \text{Xing}; q) = M_{P_p; \text{Xing}} - M_{\text{Comp}; q}$, where the first identity reaffirms that each isochrone age has been selected to match a specific combination of pulsation period and crossing number. We compute the typical companion photometric bias as:

$$\hat{M}_{P_p; \text{Xing}} = \langle -2.5 \log(1 + 10^{0.4 \Delta M_{P_p; \text{Xing}; q}}) \rangle, \quad (1)$$

where $\hat{M}_{P_p; \text{Xing}}$ denotes the mean of the distribution of $\Delta M(P_p; \text{Xing}; q)$ computed for 100 000 randomly drawn q values. Since q follows a power law (Moe & Di Stefano 2016), the distribution of ΔM obtained from this simulation also follows a power law. Consequently, the

difference between the mean and median ΔM is approximately a factor of two in all filters, with the mean giving a larger bias. Uncertainties in the slope of the power law, etc., have been neglected for the time being.

The typical photometric bias due to such wide companions translates to a fractional distance bias as:

$$d_{\text{biased}}/d_{\text{true}} = 10^{-0.2 \cdot \hat{M}_{P_p; \text{Xing}}}. \quad (2)$$

Table 3 summarizes our results obtained for different Cepheid pulsation periods and IS crossings, in V , I , and H -band as well as Wesenheit formulations. To estimate the influence on H_0 , these individual distance bias estimates must be multiplied by the fraction of stars concerned:

$$\hat{M}_{P_p; \text{wb}} = f_{wb} \cdot \hat{M}_{P_p}. \quad (3)$$

Table 3 and Figure 3 present the (very small) effect in terms of magnitude and percent distance taking into account the wide binary fraction. The largest effect is found in V -band for the shortest-period Cepheids (here: 5 d). In this worst case scenario, the bias amounts to approximately -5 mmag, or a distance error of -0.23% . Focusing on Cepheids with $P_p > 10$ d, which are most relevant for extragalactic applications, and on near-IR photometry or Wesenheit magnitudes reduces this effect to the sub-mmag level and to fractional distance errors smaller than 0.02% . Since the MW is the only *SHOES* anchor galaxy in which wide binaries may be resolved and is 1 of 3 equivalently weighted anchors, the impact of this bias enters the H_0 estimation weighted by approximately $1/3$. For a typical pulsation period of 20 d and using NIR-based Wesenheit formulation, the distance effect due to such wide companions is a mere $4 \cdot 10^{-5} = 0.004\%$, which is clearly negligible, even en route to 1% H_0 accuracy.

P_p	V-band		I-band		H-band		W_{VI}		$W_{H,VI}$	
(d)	(mmag)		(mmag)		(mmag)		(mmag)		(mmag)	
	2 nd	3 rd	2 nd	3 rd	2 nd	3 rd	2 nd	3 rd	2 nd	3 rd
For a Cepheid with a typical wide companion:										
5	-33.0	-32.4	-16.8	-16.9	-8.6	-8.8	-5.8	-6.1	-6.5	-6.7
10	-23.5	-22.4	-10.7	-10.1	-4.8	-4.4	-3.2	-2.9	-3.5	-3.2
20	-18.1	-17.0	-7.0	-6.8	-2.5	-2.5	-1.6	-1.6	-1.7	-1.7
40	-12.2	-9.4	-3.8	-3.4	-1.0	-1.2	-0.6	-0.7	-0.6	-0.8
Taking into account the wide binary fraction, $f_{wb} = 0.15$:										
5	-4.9	-4.9	-2.5	-2.5	-1.3	-1.3	-0.9	-0.9	-1.0	-1.0
10	-3.5	-3.4	-1.6	-1.5	-0.7	-0.7	-0.5	-0.4	-0.5	-0.5
20	-2.7	-2.5	-1.0	-1.0	-0.4	-0.4	-0.2	-0.2	-0.2	-0.3
40	-1.8	-1.4	-0.6	-0.5	-0.1	-0.2	-0.1	-0.1	-0.1	-0.1

Table 3. Mean photometric bias due to wide binaries. For each band and filter combination, values for second and third crossings are shown separately. $W_{VI} = I - 1.55 \cdot (V - I)$ and $W_{H,VI} = H - 0.4 \cdot (V - I)$ are the reddening-free “Wesenheit” magnitudes (Madore 1982; Soszynski et al. 2008; Riess et al. 2011) assuming $R_V = 3.1$ (Cardelli et al. 1989).

3. CEPHEIDS IN OPEN CLUSTERS

To assess the impact of a cluster-related bias, we proceed as follows. We first estimate the occurrence rate of Cepheids in clusters by reviewing the literature for cluster Cepheids in the MW, LMC, SMC, and M31, cf. §3.1. We then measure the average bias arising from cluster populations using observations of nine M31 cluster Cepheids, cf. §3.2. We finally estimate the influence of cluster-related stellar association bias on H_0 in §3.3.

3.1. Occurrence rate of Cepheids in clusters

Several previous studies aimed at investigating the effects of blending on Cepheid photometry and the distance scale have (incorrectly) asserted that Cepheids very frequently occur in open clusters based on the notion that young stars tend to reside in clusters. However, most embedded and gravitationally unbound star clusters or associations disperse within a few to a few tens of Myr (Lada & Lada 2003; Goodwin & Bastian 2006; Moeckel et al. 2012, 10% of embedded clusters with mass exceeding $150 M_\odot$ survive for 10 Myr or more). For comparison, Cepheids are several tens to a few hundred Myr old (Anderson et al. 2016a). Here we determine the occurrence rate of Cepheids in clusters, which is crucial for correctly evaluating the impact of cluster-related blending on the distance scale.

In the MW, 13 of 167 Cepheids within 2 kpc of the Sun reside in open clusters, i.e., $f_{CC,MW} = 7.8\%$ (Anderson et al. 2013). The distribution of P_p among MW cluster Cepheid periods leans heavily towards $P_p < 10$ d. This can be explained by a combination of a) evolutionary timescales, which favor the observation of short-period

in comparatively old open clusters, b) the greater frequency of low-mass stars² in stellar populations, and c) a paucity of long-period Cepheids in the Solar neighborhood. A more accurate and complete estimation of $f_{CC,MW}$ will soon be achievable using the *Gaia* survey, thanks to its astrometric and time-domain census of the Galaxy (Gaia Collaboration et al. 2016b, 2017c,b).

For short-period Cepheids, cluster membership can be much more frequent among LMC Cepheids, as evidenced by two well-studied clusters each containing up to 24 classical Cepheids have received much attention: NGC 1866 and NGC 2031 (Welch & Stetson 1993; Testa et al. 2007; Musella et al. 2016). Notably, there is no known equivalent for these clusters in the MW or the SMC, and they contain up to 8 times the number of Cepheids found in the record-holding MW cluster NGC 7790 with its 3 member Cepheids (Sandage 1958; Anderson et al. 2013). However, these well-known special cases are not representative of the typical Cepheid host cluster population in the Magellanic Clouds. The most comprehensive survey of cluster Cepheids in the LMC and SMC to date (Pietrzynski & Udalski 1999) indicates that the vast majority of Cepheid-hosting clusters in both MCs contain only one or two Cepheids, which is similar to the MW.

The LMC and SMC cluster Cepheid fractions determined by phase two of the Optical Gravitational Lensing Experiment (Udalski et al. 1997, *OGLE-II*) are

² To first order, short-period Cepheids have lower mass than longer-period Cepheids

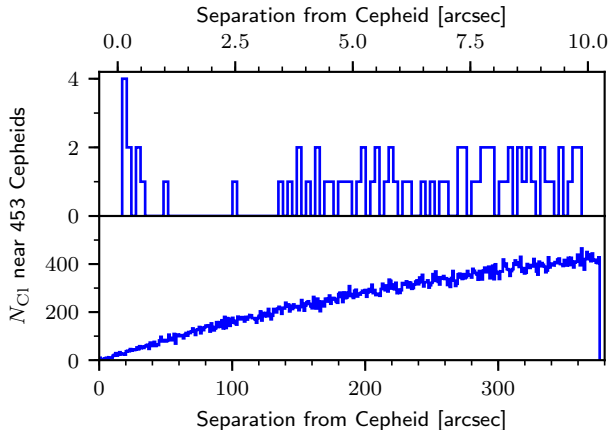


Figure 4. Number of M31 star clusters cross-matched within a given separation near M31 Cepheids (PS1 sample). The 11 known cluster Cepheids in M31 (Senchyna et al. 2015) have separations $\lesssim 1.0''$ from nearby cluster centers. A total of 535 PS1 Cepheids are found within the PHAT footprint, and 453 PS1 Cepheids have AP clusters situated at separations closer than $6.3'$ (100 *WFC/IR* pixels at 22.9 Mpc).

$f_{CC,LMC} = 15\%$ (11% not counting clusters containing more than 3 Cepheids) and $f_{CC,SMC} = 6\%$, respectively (Pietrzynski & Udalski 1999). These numbers illustrate that the LMC and SMC cluster Cepheid fraction may not be so different from the MW. In particular for long-period Cepheids ($P_{\text{puls}} > 10$ d), the clustered fraction of Cepheids is $f_{CC,LMC,longP} = 10/130 = 8\%$ in the LMC and $f_{CC,SMC,longP} = 6/86 = 7\%$ (Udalski et al. 1999a,b). While these numbers would benefit from an update based on the now completed survey of Cepheids in the Magellanic system (Soszyński et al. 2017, *OGLE-IV*), it is obvious that the occurrence of Cepheids is also comparatively uncommon in the Magellanic clouds.

The Andromeda galaxy (M31) provides a useful analog for both the MW and the *SHOES* project’s SN-host galaxies (Hoffmann et al. 2016), all of which are relatively high-mass spiral galaxies with similar (high) metallicity. To wit, $\log(\mathcal{M}_{\text{stars}}/\mathcal{M}_{\odot}) = 10.80$ (MW) and 11.1 (M31) (McMillan 2011; Tamm et al. 2012) compare to the mean stellar mass of the *SHOES* galaxies ($\log(\mathcal{M}_{\text{stars}}/\mathcal{M}_{\odot}) = 9.8$). Moreover, the average oxygen abundance is $\log[\text{O}/\text{H}] = 8.9$ for each of the MW, M31, and NGC 4258, whereas it is $\log[\text{O}/\text{H}] = 8.92$ for the *SHOES* galaxies (R+16). For comparison, the LMC has even lower mass (Kim et al. 1998, $\log(\mathcal{M}_{\text{stars}}/\mathcal{M}_{\odot}) = 9.4$) and metallicity ($\log[\text{O}/\text{H}] = 8.65$), which results in distinct differences in its Cepheid populations, such as shorter minimum periods (e.g. Anderson et al. 2016a, 2017).

The population of Cepheids in M31 is well known thanks to the Pan-STARRS survey (Kodric et al. 2013,

PS1). High-quality deep *HST* imaging in multiple passbands of approximately one third of M31’s disk is available via the Panchromatic Hubble Andromeda Treasury project (Dalcanton et al. 2012, PHAT). M31 star clusters have been identified by the Andromeda Project (Johnson et al. 2015, AP), and 11 Cepheid-hosting clusters have been reported (Senchyna et al. 2015), cf. Tab. 4. Cross-matching all PS1 Cepheids with the PHAT source catalog (Williams et al. 2014), we identify 535 PHAT sources within angular separations of typically less than $0.2''$ (maximum separation $1.2''$) from the PS1 input positions. Given the 11 M31 cluster Cepheids, this yields a fraction of clustered Cepheids of $f_{CC,M31} = 11/535 = 2.1\%$ within the PHAT footprint, which is a factor of 3 to 4 lower than the MW and LMC/SMC fractions established above.

For the time being, we cannot determine whether this estimate of $f_{CC,M31}$ a) reflects the true fraction of clustered Cepheids in M31, b) is subject to observational selection effects, or c) is representative of distant SN-host galaxies. Variations of f_{CC} among galaxies are to be expected given the above comparison between MW, LMC, and SMC, and may be explained e.g. by the dependence of cluster dispersal timescales, which depend on various factors, including galactic potentials and the presence of molecular clouds. However, it is reasonable to expect a clustered Cepheid fraction in the lower percent range, given the ~ 10 Myr timescale for cluster dissociation and typical ages of 50 – 75 Myr for 20 – 10 d Cepheids.

Given the aforementioned similarities between M31 and SN-host galaxies—in particular the external view and galaxy type—we in the following consider $f_{CC,M31} = 2.1\%$ as an *effective* cluster Cepheid fraction for our estimation of stellar association bias by clusters. Although $f_{CC,M31}$ is considerably smaller than the MW fraction, we note that it has been established based on a much larger number of Cepheids (535 vs. 167). Moreover, determining cluster membership in the MW is challenging due to uncertain line of sight distances and different observational biases applying to Cepheids and clusters as a function of distance (for details, cf. Anderson et al. 2013). Adopting a higher fraction linearly affects the result of the total bias, cf. §3.3. We discuss limitations and uncertainties related to f_{CC} in §4.2.

3.2. Measuring Cluster Cepheid Bias in M31

In contrast to the synthetic approach adopted for binaries, we estimate the stellar association bias due to clusters empirically using observations of M31 obtained via the PHAT project (Dalcanton et al. 2012). M31 and PHAT data provide a suitable empirical base for this estimation, since clusters in M31 are sufficiently spatially

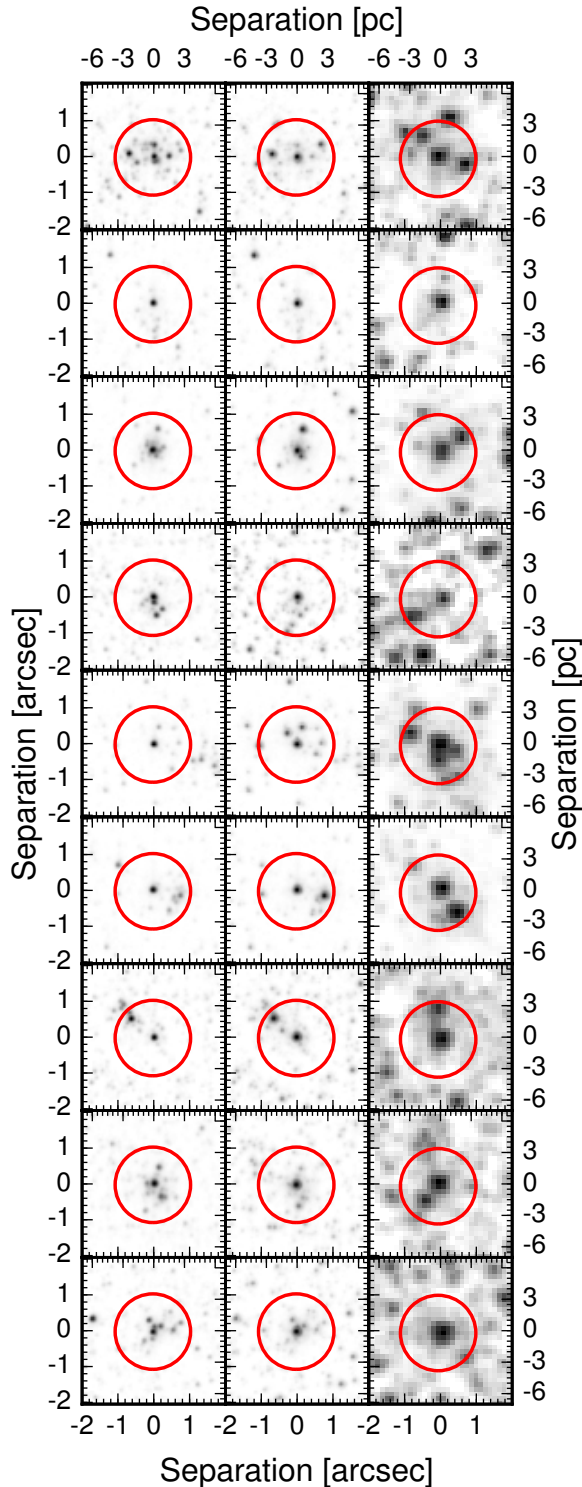


Figure 5. Postage stamps of the 9 Cepheids located near clusters in M31. For every star (sorted by increasing P_p and M31CC-ID, cf. Tab. 4), we show cutouts from the F475W, F814W, and F160W images, with wavelength increasing from left to right. The red circle indicates the area over which the cluster contributes light and has radius $r_{\text{apt}} = 1.05''$. Note that F475W and F814W have identical orientation and a finer plate scale ($0.05''/\text{pix}$ ACS compared to WFC3/IR channel $0.13''/\text{pix}$, which is also rotated.)

resolved, optical and near-IR images are available in the *HST* filter system, and M31 is an appropriate analog for comparison with SN-host galaxies. Moreover, basing this estimate on observations implies that certain typical observational systematics such as overlapping stellar populations, variable background, and other noise sources are naturally included in the estimation.

To measure the blending bias due to clusters, we downloaded the original PHAT observations from MAST³ and proceeded as follows. Note that we have measured photometry ourselves, and did not rely on published magnitudes (Williams et al. 2014).

Nine of the eleven known M31 cluster Cepheids (Senchyna et al. 2015) have been identified as fundamental-mode pulsators (Kodric et al. 2013), whereas the pulsation mode was not identified for two others. One Cepheid with unidentified pulsation mode, PSO-J011.6374+42.1393, is likely pulsating in the fundamental mode ($P_p = 7.928$ d), since the longest-known period of an overtone pulsator in the MW is 7.57 d (Baranowski et al. 2009). The other Cepheid with unidentified pulsation mode, PSO-J011.4279+41.8642 ($P_p = 6.08$ d) was located too close to the ACS chip gap to measure photometry using extended apertures described below. Unfortunately, PSO-J011.0696+41.8571, was not observed in F160W. Thus, we have included 9 Cepheids for estimating the typical blending due to M31 clusters. This sample is listed in Tab. 4 together with identifiers adopted for the present work that are ordered by pulsation period.

Correctly identifying the Cepheids in the HST images is crucial, since their astrometry is based on the lower spatial resolution of the PanSTARRS survey ($0.258''/\text{pixel}$). To this end, we assumed that the Cepheid should be the brightest object within $1''$ from the PS1 Cepheid’s position in the F814W image. This approach is a reasonable assumption due to the evolved state and yellow color of the Cepheid and has been shown to yield a narrow near-IR M31 PLR with low dispersion (Riess et al. 2012). Nearby red giants of similar luminosity may rival or outshine the Cepheid in F160W, whereas hot stars may approach the Cepheid’s brightness in F475W. We inspected all F475W, F814W, and F160W postage stamp cut outs centered on the Cepheid positions to ensure that the relative contrast of nearby stars would behave as expected for a Cepheid. Figure 5 shows these postage stamps.

³ <http://mast.stsci.edu>

M31CC-ID	Cepheid PS1 ID	AP ID	P_p (d)	a_{Cep} (Myr)	p_{Cl}
M31CC-01	PSO-J011.4286+41.9275	477	4.582	122	0.99
M31CC-02	PSO-J011.6227+41.9637	3928	6.213	101	0.87
M31CC-03	PSO-J011.6374+42.1393	2831	7.928	88	0.91
M31CC-04	PSO-J010.9769+41.6171	3050	8.829	82	0.85
M31CC-05	PSO-J011.6519+42.1286	2113	15.429	59	0.98
M31CC-06	PSO-J011.7119+42.0449	2587	17.180	56	0.83
M31CC-07	PSO-J011.0209+41.3162	2967	19.566	51	0.66
M31CC-08	PSO-J011.2797+41.6217	1082	26.499	43	0.91
M31CC-09	PSO-J011.3077+41.8500	1540	35.750	36	0.98
Known M31 cluster Cepheids that could not be studied, see text					
—	PSO-J011.4279+41.8642	too close to <i>HST/ACS</i> chip gap			
—	PSO-J011.0696+41.8571	no F160W observation			

Table 4. Table of M31 cluster Cepheids (Senchyna et al. 2015) included in this study. We present a short-hand identifier in addition to the original Cepheid (Kodric et al. 2013, PS1) and cluster identifiers (Johnson et al. 2015, Andromeda Cluster Project). P_p denotes the PS1 pulsation period. Ages are inferred using period-age relations for solar-metallicity Cepheid models that include rotation (Anderson et al. 2016a). Column p_{Cl} represents a probability of the cluster existing (cf. Andromeda Project); this is however not a cluster membership probability for the Cepheid.

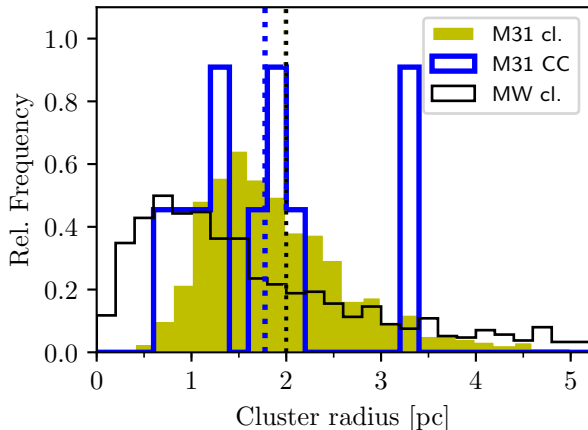


Figure 6. Relative frequency of cluster radii in M31 (Johnson et al. 2015, yellow area) and the Milky Way (Dias et al. 2002, black line, restricted to ones within 2 kpc of the Sun), and the relative frequency of cluster radii among Cepheid host clusters in M31 (Senchyna et al. 2015, thick blue line). The mean cluster radii in M31 and the MW are virtually identical, $\langle r_{\text{cl}} \rangle = 2.0$ pc. The mean radius of M31 Cepheid host clusters is 1.8 pc.

3.2.1. Measuring photometric bias due to clusters

There are three separate contributions to the flux in an aperture centered on a cluster Cepheid: 1) the Cepheid flux, 2) the resolved cluster flux, and 3) the average unassociated background. To estimate the isolated resolved cluster flux, we first measure and remove the curve of growth for point sources matched to a small,

$r=1$ pixel, aperture centered on the Cepheid. The background is then statistically measured as the mean of a larger-than-the-cluster annulus, and subtracted from the curve of growth. This leaves an estimate of the cluster flux.

We measure each image’s curve of growth $m_{2\text{px}} - m_{N\text{px}}$ using a series of apertures of increasing radius, starting from $r = 1$ pixel to $r = 1.5''$ (5 pc) for ~ 1000 stars. The 5 pc radius was inspired by typical cluster radii, cf. Fig. 6 (Dias et al. 2002; Johnson et al. 2015), and the feasibility of measuring photometry in extended apertures in the PHAT images. Figure 6 shows the distribution of physical sizes of MW and M31 clusters, with the M31 Cepheid-hosting clusters highlighted. The apparent difference in cluster radii is likely due to the inhomogeneous definition of cluster radii in the Galactic catalog (Dias et al. 2002), whereas a consistent definition applies to M31 clusters. The mean cluster radius of both distribution is ~ 2 pc, which translates to angular sizes of $0.53''$, $0.054''$, $0.018''$, and $0.010''$ at the distances corresponding to M31, NGC 4258, the average of the *SHOES* SN-host galaxies in R+16 (22.9 Mpc), and the farthest R+16 galaxy: UGC 9391 (38.5 Mpc).

We define the sky background as the *mean* flux in an annulus just outside the largest aperture used to measure the curve of growth ($1.5''$ to $2.5''$). We employ the mean rather than the median in order to be sensitive to background stars in addition to the sky level, which in itself would be probed more robustly via the median.

We then estimate the mean flux level of the Cepheid plus cluster stars within the aperture by subtracting the mean flux of sources and non-sources in the outer annulus from the aperture region containing the Cepheid and cluster stars. This somewhat noisy estimate of the mean Cepheid plus cluster flux level depends on the brightness and number of stars that lie within the aperture or annulus. An additional source of noise is the random phase magnitude estimate of the Cepheid, for which we do not correct here.

To isolate the extra flux contributed by cluster stars (without the Cepheid), we subtract the curve of growth measured within the series of apertures from the mean Cepheid plus cluster flux. This provides us with the cluster flux contributions as a function of angular separation from the Cepheid in each of the photometric passbands considered.

Figure 7 shows the resulting estimate of the cumulative cluster flux contribution as a function of separation from the Cepheid for each of the 9 cluster Cepheids. We have defined the blending bias for each filter as

$$\Delta M = M_{\text{Cep}} - M_{\text{Cl+Cep}}, \quad (4)$$

where M denotes the magnitude in the filter of interest and ΔM is negative when a light contribution beyond the background is present. Table 5 lists the inferred biases for all 9 Cepheids. Note that the estimate of the cluster flux can be negative (positive ΔM) due to its statistical nature, e.g., if the cluster flux is small and its location statistically sparser than the nearby (annulus) environment.

Figure 7 shows that ΔM_{F475W} is positive at most cluster radius apertures with a mean (median) of 0.79 ± 0.15 (0.72) mag at an aperture corresponding to $r_{\text{apt}} = 3.8$ pc (cf. below). This agrees very well with the expectation that young clusters contain many hot stars (cf. also §4.2). In F814W the mean (median) $\Delta M_{\text{F814W}} = 0.45 \pm 0.14$ (0.43) mag. For F160W, the mean (median) $\Delta M_{\text{F160W}} = 0.39 \pm 0.16$ (0.43) mag, which is similar to the average bias in F814W, albeit with greater noise due to the stronger influence of the red giants at longer wavelengths. Again, the postage stamps (Fig. 5) illustrate the blue nature of the (very centrally concentrated) cluster population dominated by hot stars, whereas the field red giants (more widely distributed) become dominant sources in F160W.

Figure 8 shows the mean cluster light contribution as a function of separation obtained averaging the 9 curves of growth in Fig. 7. On average, noisy field star contamination cancels out and we recover a smoothly increasing cluster light contribution as a function of separation. From this average curve of growth, we find that

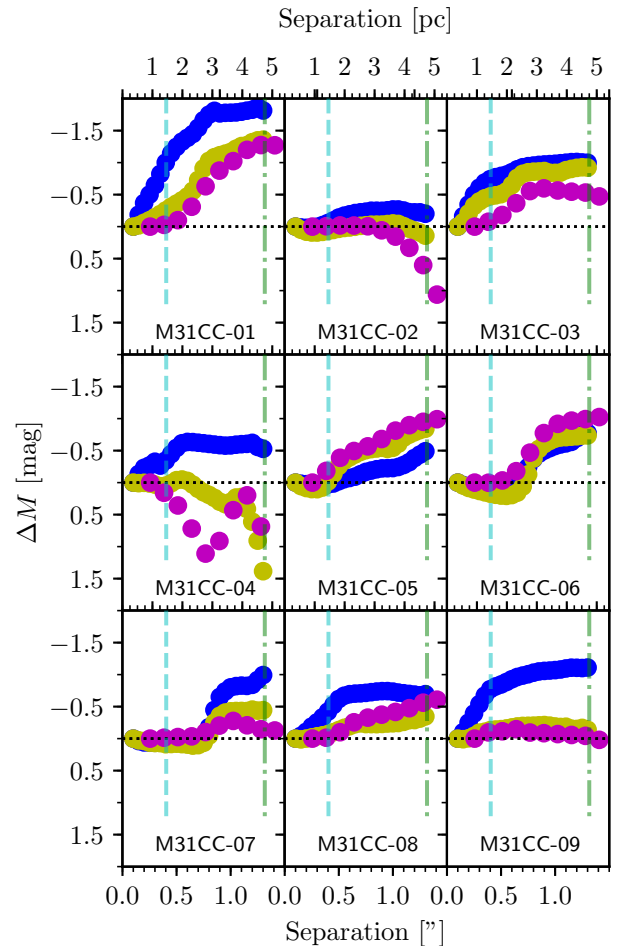


Figure 7. Cumulative light contribution due to cluster stars for each M31 cluster Cepheid considered, cf. §3.2. Colors represent different filters: F475W (blue), F814W (yellow), F160W (magenta).

the cluster light contribution flattens off at a separation of about $r_{\text{apt}} = 1.05'' \equiv 3.8$ pc. This distance corresponds to nearly twice the average cluster (half-light) radius of M31 open clusters, cf. Fig. 6. We thus adopt $r_{\text{apt}} = 3.8$ pc as the typical area over which a cluster contributes light to a Cepheid’s photometry. Table 5 lists the mean bias estimates at $r_{\text{apt}} = 3.8$ pc.

We compute reddening-free Wesenheit magnitudes (Madore 1982), using combinations of optical as well as optical and near-IR photometry. The F160W observations yield H -band magnitudes. We estimate $V - I$ color by interpolation using observed F475W-F814W color space and the color-color (F475W-F814W vs. F555W-F814W) space defined by a PARSEC isochrone⁴ (Marigo et al. 2017) computed for an age of 50 Myr and solar

⁴ <http://stev.oapd.inaf.it/cmd>

metallicity, since the PHAT project did not observe in F555W (V -band).

Table 5 lists the measured values of ΔM —i.e., the change in apparent magnitude due to extra flux—for each cluster Cepheid and passband or Wesenheit magnitude separately, as well as the mean of all 9 cluster Cepheids including standard error and median. Intriguingly, we find a nearly vanishing cluster bias in the optical Wesenheit magnitude W_{VI} at the typical cluster aperture $r_{\text{apt}} = 3.8$ pc. The integrated cluster contribution in $V - I$ is evidently just blue enough to compensate the I -band bias if it is multiplied with the reddening law. Moreover, we find evidence of mass segregation in the young Cepheid-hosting clusters given that the cluster stars within ~ 1.5 pc appear to be bluer than the stars farther away from the center (cf. yellow upward triangles in Fig. 8). $\Delta M_{W,H,VI}$, which is particularly relevant for the measurement of H_0 is reduced compared to the bias measured using F160W exclusively. For a typical cluster Cepheid, we thus find a brightening by $\langle \Delta M_{W,H,VI} \rangle = 0.30 \pm 0.18$ mag due to the integrated cluster population. If F160W observations are used without a color term, the typical bias is $\langle \Delta M_{F160W} \rangle = 0.39 \pm 0.16$ mag.

3.3. Cluster bias and H_0

We estimate the impact of stellar association bias by cluster populations on H_0 by multiplying the effective clustered Cepheid fraction and the typical cluster bias estimated in §3.1 and §3.2 above:

$$\hat{M}_{\text{CC}} = f_{\text{CC}} \cdot \langle \hat{M} \rangle, \quad (5)$$

where $\langle \hat{M} \rangle$ is the mean bias listed in Tab. 5 and $f_{\text{CC}} = 0.021$ the effective fraction of clustered Cepheids as observed in M31. We thus obtain for the bias in terms of distance modulus for a given distant galaxy:

$$\Delta\mu_{F160W} = 0.021 \cdot (-0.39 \pm 0.16) \text{ mag} = -0.008 \pm 0.003 \text{ mag} \quad (6)$$

$$\Delta\mu_{W_{H,VI}} = 0.021 \cdot (-0.30 \pm 0.18) \text{ mag} = -0.006 \pm 0.004 \text{ mag} \quad (7)$$

Propagating this bias to the determination of H_0 , it must be kept in mind that stellar association bias arises due to the distance-dependent ability to spatially resolve clusters. Star clusters are barely resolved at the distance of NGC 4258 (7.6 Mpc) or M101, since typical cluster half-light radii of 2 pc correspond approximately to the plate scale of *HST/ACS*. Since NGC 4258 is similarly affected by cluster light contributions as the 19 *SHOES* SN-host galaxies, the stellar association bias does not apply in this galaxy, especially when working with F160W magnitudes. However, for the two other

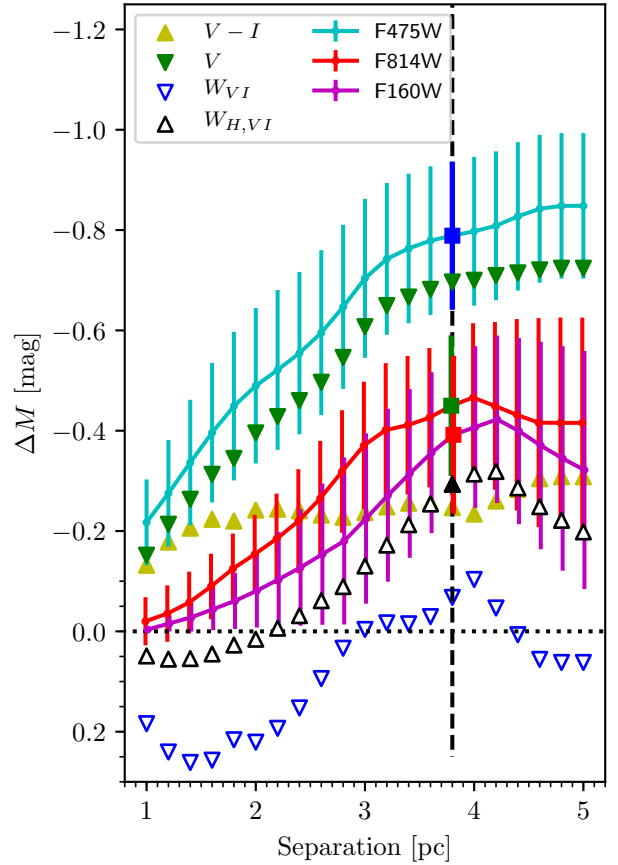


Figure 8. Mean bias vs separation as obtained from the 9 individual cluster Cepheids shown in Fig. 7. W denotes reddening-free Wesenheit magnitudes computed using optical photometry (W_{VI}) as well as combined near-IR and optical photometry ($W_{H,VI}$), cf. §3.2. The dashed vertical line shows the separation $r_{\text{apt}} = 3.8$ pc at which the cluster contribution levels off. Differently colored larger symbols are drawn here to illustrate that this ΔM is used to evaluate stellar association bias due to clusters. $V - I$ color is estimated by color-color (F475W-F814W vs F555W-F814W) interpolation using a 50 Myr solar-metallicity isochrone. The run of $V - I$ (yellow upward triangles) suggests evidence of mass segregation in the young Cepheid-hosting clusters. Intriguingly, optical Wesenheit magnitudes appear to be highly insensitive to the cluster light contribution. Combined near-IR and optical Wesenheit magnitudes are slightly less sensitive to cluster light contributions than near-IR data alone.

anchors used to set up the distance ladder (MW and LMC), this bias does apply. Adopting the three anchors recommended by R+16 (MW, LMC, NGC 4258) and weighting them equally⁵, it follows that the impact of stellar association bias should be weighted by two thirds. Thus, for the distance scale as a whole, we esti-

⁵ We have verified that this is a good approximation by running the global optimization as described in R+16

M31CC ID	ΔM_{F475W} (mag)	ΔM_{F814W} (mag)	ΔM_{F160W} (mag)	ΔM_{VI} (mag)	$\Delta M_{W,VI}$ (mag)	$\Delta M_{W,HVI}$ (mag)
M31CC-01	-1.7847	-1.2192	-1.0401	-0.3929	-0.6102	-0.8829
M31CC-02	-0.2671	-0.0400	0.1732	-0.1696	0.2229	0.2410
M31CC-03	-0.9905	-0.8469	-0.5631	-0.1120	-0.6732	-0.5183
M31CC-04	-0.5931	0.2327	0.4085	-0.5624	1.1044	0.6335
M31CC-05	-0.2460	-0.6125	-0.8206	0.2150	-0.9457	-0.9066
M31CC-06	-0.5973	-0.7054	-0.9231	0.0714	-0.8160	-0.9516
M31CC-07	-0.8209	-0.4311	-0.2697	-0.2787	0.0010	-0.1582
M31CC-08	-0.7188	-0.2448	-0.4225	-0.3349	0.2742	-0.2885
M31CC-09	-1.0808	-0.1819	-0.0694	-0.6094	0.7627	0.1744
mean bias	-0.7888	-0.4499	-0.3918	-0.2415	-0.0756	-0.2952
standard mean error	0.1476	0.1401	0.1569	0.0860	0.2294	0.1788
median bias	-0.7188	-0.4311	-0.4225	-0.2787	0.0010	-0.2885

Table 5. Cluster light contribution for 9 cluster Cepheids in M31, cf. §3.2. Negative ΔM indicates brightening due to the cluster. M31CC ID is the object number assigned in this paper, cf. Tab. 4. $\Delta M_{VI} = \Delta M_{F555W} - \Delta M_{F814W}$ is estimated by interpolating the observed $\Delta M_{F475W} - \Delta M_{F814W}$ color in color-color space (F475W-F814W vs F555W-F814W) defined by a BASTI isochrone with age = 50 Myr and Solar metallicity. $\Delta M_{W,VI} = \Delta M_{F814W} - 1.55 \cdot \Delta M_{VI}$ and $\Delta M_{W,HVI} = \Delta M_{F160W} - 0.4 \cdot \Delta M_{VI}$ quantify the bias in the reddening-free Wesenheit magnitudes. The mean and median shown in the bottom two lines are computed column-wise for all 9 Cepheids.

mate the effective bias in distance modulus to be:

$$\Delta \mu_{F160W} = 2/3 \cdot (-8 \pm 3) \text{ mmag} = -5 \pm 2 \text{ mmag} \quad (8)$$

$$\Delta \mu_{W,HVI} = 2/3 \cdot (-6 \pm 4) \text{ mmag} = -4 \pm 3 \text{ mmag} \quad (9)$$

These distance modulus differentials translate to fractional distance bias of -0.25% and -0.19% in F160W and $W_{H,VI}$, respectively, implying values of the Hubble constant to be overestimated by $\Delta H_0 = 0.18$ and $0.14 \text{ km s}^{-1} \text{ Mpc}^{-1}$ assuming $H_0 = 73.24 \text{ km s}^{-1} \text{ Mpc}^{-1}$ (R+16). Cluster bias is thus at least an order of magnitude larger than the bias due to wide binaries (§2), because clusters contain hundreds to thousands of stars, which by far outweighs the fact that the (effective) occurrence rate of Cepheids in clusters is 10 times lower than the occurrence of wide binaries.

Correcting for stellar association bias thus leads to $H_0 = 73.06 \pm 1.76 \text{ km s}^{-1} \text{ Mpc}^{-1}$, which remains (nearly unchanged) 3.3σ larger than H_0 determined by *Planck* (Planck Collaboration et al. 2016, $66.93 \pm 0.62 \text{ km s}^{-1} \text{ Mpc}^{-1}$). Thus, stellar association bias does not reconcile the observed tension between the distance-scale and CMB-based values of H_0 .

4. DISCUSSION

4.1. Cepheids in binary systems and the distance scale

Binary companions affect the PLR calibration in at least two ways: one, by providing additional flux and

two, by biasing parallax measurements for Galactic Cepheids, if orbital motion is not taken into account in the astrometric model. Companions with reasonably short orbital periods (a couple to a few years) capable of significantly affecting parallax are detectable using precision radial velocity measurements (Anderson et al. 2016b), even if such companion stars are too faint to leave a clear photometric signature (Anderson et al. 2015; Gallenne et al. 2016). In most such cases, *Gaia* (Gaia Collaboration et al. 2016c, 2017a) astrometry should be sufficient to solve for orbital motion, in particular when independent evidence of a companion’s presence is available a priori.

In general, the “parasitic” flux contributed by companion stars cannot be corrected individually, although this may be possible statistically. As shown in §2, additional flux contributed by wide binaries has a negligible effect on the distance scale, in particular when working with near-IR data as well as Wesenheit magnitudes (thanks to the color difference between Cepheids and typical companions). However, a larger bias for the distance scale would arise if the Galactic PLR calibration were based exclusively on single Cepheids, while extragalactic Cepheids were not selected accordingly. Bias due to binaries would increase in such a case primarily because f_{wb} would have to be replaced with the total binary fraction of Cepheids. Not correcting for differences in preferred mass ratios in closer-in binary systems

(Moe & Di Stefano 2016), Tab. 3 provides a useful upper limit to this effect, which would be approximately $\Delta M_{W_{H,VI}} = 0.6 \cdot -1.7 = -1.0$ mmag, i.e., -0.05% in distance for 20 d Cepheids.

Our results suggest a period-dependent contrast between Cepheids and their companions, which leads to a predicted, albeit small, non-linearity in the PLR slope of real Cepheid populations consisting of both singles and multiples. Using the numbers listed Tab. 3 and assuming a total binary fraction of $f_{\text{bin}} = 60\%$, we find a period-dependent deviation (computed as the difference between 5 d and 40 d Cepheids) from the single-star PLR of -13 mmag in V -band, whereas the deviation reduces to -7.8 , -4.6 , -3.1 , and -3.5 mmag in I - and H -band and the Wesenheit magnitudes W_{VI} and $W_{H,VI}$. These numbers underline that non-linearity due to binaries is a small effect, even if they are upper limits, since closer-in binaries favor smaller mass ratios than wide binaries (Moe & Di Stefano 2016). Observational evidence for PLR non-linearity has been disputed in the literature, indicating a weak phenomenon. However, PLR non-linearity appears to be more readily observed in optical passbands than in near-IR or Wesenheit magnitudes (Tammann & Reindl 2002; Sandage et al. 2004; Ngeow & Kanbur 2006; Inno et al. 2013; Bhardwaj et al. 2016). These two facts seem to corroborate an origin of PLR non-linearity linked to multiplicity, since the contrast between Cepheids and their companions depend on wavelength and are significantly smaller in V -band than in H -band. However, given the disputed nature of PLR non-linearity in the literature, it is clear that further study is required to conclude in this matter.

4.2. Cepheids in clusters and the distance scale

As shown in §3.3, contamination by cluster populations dominates the distance scale bias due to stellar association, despite the rare occurrence of Cepheids in clusters. The uncertainty on this effect is dominated by the fraction of clustered Cepheids, which we found to be 2% in M31, and between 6 – 8% in the other galaxies considered (MW, LMC, SMC), in particular when considering long-period Cepheids ($P_{\text{puls}} > 10$ d), cf. §3.1. Since f_{CC} enters linearly in Eq. 5 and is uncertain (or galaxy-dependent) by a factor of 2 – 4, the estimates of stellar association bias due to clusters are uncertain by an analogous factor.

f_{CC} is subject to a complex mixture of completeness issues and selection effects, which may depend on the galaxy being considered. In the MW, for instance, a main issue is host cluster detection at typical Cepheid distances and distinguishing real cluster membership from chance superposition (Anderson et al.

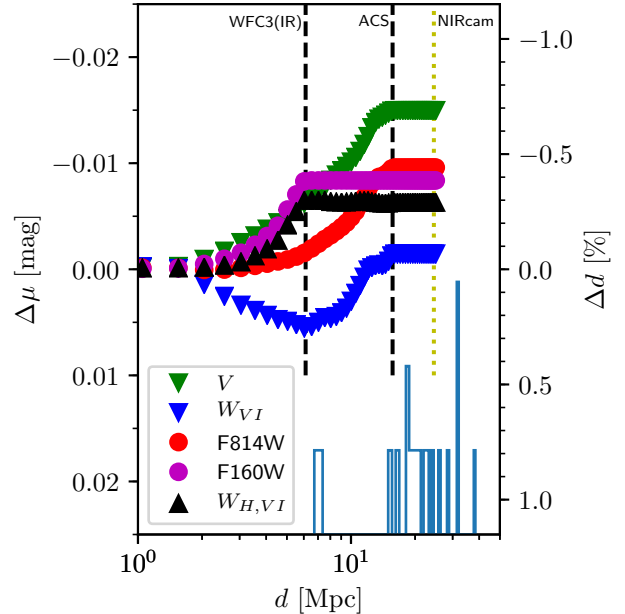


Figure 9. Combined stellar association distance bias due to both binaries and clusters ($\Delta\mu$ or Δd) incurred within a single pixel as a function of the distance at which a galaxy of interest is located. The curves level off at the distance where the typical physical cluster size (3.8 pc, cf. §3.2.1) is equal to the size of a single pixel given the WFC3(IR) and ACS plate scales (cf. vertical dashed lines). The dotted yellow line indicates the distance at which one JWST/NIRcam pixel corresponds to a physical scale of 3.8 pc. The histogram at the bottom shows the distribution of *SH0ES* SNIa-host galaxies (R+16). M101 is the sole SN-host galaxy for which resolving Cepheid host clusters may be feasible. The positive $\Delta\mu$ in the W_{VI} filter combination is a consequence of the typical cluster color and the definition of this Wesenheit magnitude. Interestingly, the total stellar association bias is very near 0 in the optical ($V - I$) Wesenheit magnitude.

2013). Thankfully, *Gaia* will soon significantly improve on this situation by providing a homogeneous census of both clusters and Cepheids within several kpc from the Sun. The Magellanic System’s lower metallicity (compared to *SH0ES* galaxies) and possibly peculiar star formation history may alter f_{CC} compared to “normal” spiral galaxies. This is particularly evident when considering clusters such as NGC 1866 containing more than 20 (short-period) Cepheids, although the clustered fraction of long-period ($P_{\text{puls}} > 10$ d) LMC Cepheids is much lower (8%).

Estimating an expected f_{CC} using an order of magnitude calculation is not straightforward, since it would require assumptions on several unknown quantities, including notably a) the fractions of stars born in gravitationally bound and unbound clusters and b) the survival rate for clusters (in a given galaxy). Both issues are complex considering the diversity of star clusters and their

host galaxies. Among other things, cluster survivability depends on individual cluster properties (e.g. mass or number of stars, which differ by approx. 2 orders of magnitude among clusters) and the frequency and intensity of tidal interactions with molecular clouds (Friel 2013, and references therein). Differences in galactic potentials and partners for interactions may thus explain the differences found in f_{CC} among the MW, LMC, SMC, and M31.

An interesting point to consider is whether the occurrence of Cepheids in clusters is biased in any particular direction, e.g. whether cluster mass or luminosity are factors. On the one hand, M31 cluster completeness is primarily a question of cluster mass (Johnson et al. 2015, $\sim 50\%$ completeness for $500M_{\odot}$), i.e., lower mass clusters are less likely to be discovered. On the other hand, however, Cepheids are intrinsically very bright objects, so that the detection of clusters by the Andromeda Project (Johnson et al. 2015) may have been more efficient at detecting clusters near Cepheids (and other supergiants) than in other regions. AP cluster mass estimates (Johnson et al. 2016) yield a median mass of Cepheid host clusters of $850M_{\odot}$, whereas the median AP cluster mass is $1300M_{\odot}$. At face value, this difference suggests a higher than usual efficiency of discovering clusters near supergiant stars, although the small number statistics and mass uncertainties require a cautious interpretation. Nevertheless, these numbers certainly do underline that Cepheids are not preferentially found in higher mass clusters. If there is a physical reason for Cepheids to reside in lower-than-average mass clusters, then the incompleteness of the AP cluster catalog may partially explain why the clustered Cepheid fraction in M31 is lower than in the other galaxies considered. However, cluster disruption timescales differ by orders of magnitude among different galaxies, or even within different regions inside a given galaxy (Boutloukos & Lamers 2003; de Grijs et al. 2003), so that the low f_{CC} of M31 may just be a property of this particular galaxy.

Of course, the relevant issue for the distance scale as a whole would be what *effective* value of f_{CC} applies on average among SN-host galaxies. Further study and observations targeting Cepheid-hosting clusters in additional galaxies are required to provide a more definitive answer to this important question.

Figure 10 shows normalized distributions of AP cluster integrated luminosities and highlights known Cepheid host clusters for optical and near-IR passbands. No selection based on age was made when preparing these histograms. Overall, we confirm the result of §3.2.1 that Cepheid host clusters have fairly hot member stars, i.e.,

have blue integrated colors, cf. Fig. 5. The blue intrinsic color of Cepheid host clusters may thus be exploited to identify extragalactic Cepheids that are blended with host clusters. Short wavelength (U or B -band) observations of Cepheids in *SHOES* galaxies would be useful for identifying such cluster contamination.

Cepheids in the distant *SHOES* galaxies are subject to blending-related detection bias, whereby a host cluster’s flux contribution decreases a Cepheid’s light amplitude, possibly preventing its discovery. This would affect primarily low-amplitude ($P_p \sim 10$ d) and short-period cluster Cepheids and reduce the *effective* cluster Cepheid fraction relative to the real occurrence rate of Cepheids in clusters. Since any existing cluster populations are unresolved in *SHOES* galaxies, Cepheids residing in clusters would also appear brighter than the bulk of Cepheids (by about 0.3 mag in H -band, cf. Tab. 5) that define a particular galaxy’s Leavitt law. Given the observed PLR scatter in H -band of 0.3 – 0.4 mag (R+16), a commonly applied $\sim 3\sigma$ sigma-clipping procedure around a PLR (Riess et al. 2011; Kodric et al. 2013; Wagner-Kaiser et al. 2015; Hoffmann et al. 2016, R+16) would not remove typical cluster Cepheids.

Finally, we note that occasional chance blending by clusters during artificial star tests does not significantly compensate for stellar association bias. Based on a cross-match (cf. Fig. 4) of AP-clusters located within 6.3 arcmin (corresponds to 100 *WFC3/IR* pixels at the mean *SHOES* SN-host distance) of PS1 Cepheids, we compute a fractional area⁶ occupied by clusters of 2.2×10^{-5} , two orders of magnitude smaller than f_{CC} .

4.3. Mitigating Stellar Association Bias

Thanks to the upcoming releases of *Gaia* parallaxes, the calibration of the Leavitt law in the MW will experience a quantum leap in accuracy, and harnessing *Gaia*’s power to push toward an H_0 measurement to within 1% accuracy requires mitigation of any intervening uncertainties and biases. Here, we have estimated that stellar association bias amounts to approximately 0.2% of H_0 . Hence, stellar association bias shall not prevent a measurement of H_0 to within 1%, despite the stated uncertainty involving the effective fraction of Cepheids occurring in clusters.

Nonetheless, we identify a few strategies for avoiding or mitigating stellar association bias below.

1. MW Cepheids in binary (multiple) systems should not be excluded from local PLR calibrations, since no analogous selection is made in the case of ex-

⁶ Computed using twice the effective AP cluster radii

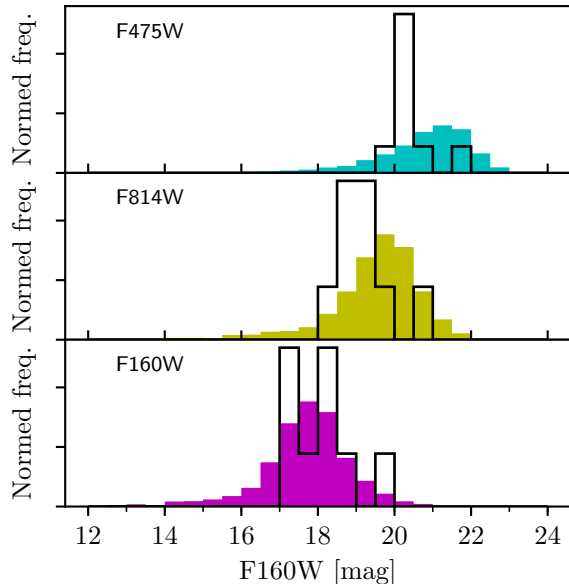


Figure 10. Luminosities of all PHAT clusters (Johnson et al. 2015, filled in step histograms) compared to the luminosities of 9 Cepheid-hosting clusters in M31 (black step histograms).

tragalactic Cepheids for which no knowledge regarding their multiplicity is available. This is equivalent to assuming a universal binary fraction for Cepheids. Calibrating the MW PLR exclusively using single Cepheids implies a passband-dependent slope difference between the MW and extragalactic Leavitt laws, cf. §4.1.

2. Additional independent distance estimates to SN-host galaxies would be extremely useful, provided they are insensitive to blending. This is the case for parallax measurements of the water megamaser in NGC 4258 (Humphreys et al. 2013), for instance. However, it remains to be seen how many more such maser distances can be determined.
3. Observations in short optical passbands may prove to be useful for identifying Cepheids residing in comparatively young clusters. Stellar association bias would be very effectively mitigated, if cluster Cepheids could thus be identified and excluded from the analysis.
4. Short wavelength photometric data of the SN-host galaxy M101 would be particularly useful to obtain a second distance-scale relevant estimate the effective fraction of clustered Cepheids, f_{CC} , cf. Fig. 9.

5. SUMMARY

We have investigated the effect of stellar association bias on Cepheid distance measurements and the Hubble constant. Understanding this and other possible biases affecting the distance scale is crucial for measuring H_0 with an accuracy of 1% to elucidate dark energy and understand the origin of the observed *tension* between distance scale and CMB-based determinations of H_0 .

We have estimated stellar association bias in two parts. First, we have used state-of-the-art stellar evolution models (Ekström et al. 2012) and detailed statistics on the multiplicity fraction of intermediate-mass stars to investigate the effect of wide binaries. We show that wide binaries have a negligible effect of approximately 0.004% on H_0 .

Second, we have used deep *HST* imaging of M31 provided by the PHAT survey (Dalcanton et al. 2012) to measure the photometric contribution by typical Cepheid hosting clusters in photometric passbands commonly used to construct the distance scale. We have further considered the clustered fraction of Cepheids, f_{CC} in different galaxies (MW, LMC, SMC, M31). Despite being uncertain by a factor of two or more, f_{CC} is on the order of a couple to a few percent, implying a small overall effect of stellar association bias on the distance scale.

We estimate the H_0 bias due to star clusters at approximately -0.25% and -0.19% , respectively using H -band (F160W) observations and Wesenheit magnitudes $W_{H,V1}$ based on F160W, F555W, and F814W observations. These values assume that M31’s $f_{CC} = 2.1\%$ applies to all SN-host galaxies and our bias estimate scales linearly with f_{CC} .

We have thus shown that stellar association bias does not prevent achieving 1% accuracy on H_0 . Given the uncertainty on f_{CC} , however, further research into this area is warranted. Short optical wavelength observations of nearby Cepheid hosting galaxies would be particularly beneficial to this end.

We thank Stefano Casertano for useful discussions.

Based on observations made with the NASA/ESA Hubble Space Telescope, obtained from the data archive at the Space Telescope Science Institute. STScI is operated by the Association of Universities for Research in Astronomy, Inc. under NASA contract NAS 5-26555.

This research made use of NASA’s Astrophysics Data System Bibliographic Services and Astropy, a community-developed core Python package for Astronomy (Astropy Collaboration et al. 2013).

Facilities: HST(ACS and WFC3)

REFERENCES

- Abbott, B. P., Abbott, R., Abbott, T. D., & et al. 2017, ArXiv e-prints, arXiv:1710.05835
- Addison, G. E., Watts, D. J., Bennett, C. L., et al. 2017, ArXiv e-prints, arXiv:1707.06547
- Anderson, R. I., Ekström, S., Georgy, C., et al. 2014, *A&A*, 564, A100
- Anderson, R. I., Ekström, S., Georgy, C., Meynet, G., & Saio, H. 2017, in *European Physical Journal Web of Conferences*, Vol. 152, *Wide-Field Variability Surveys: A 21st Century Perspective – 22nd Los Alamos Stellar Pulsation – Conference Series Meeting*, 06002
- Anderson, R. I., Eyer, L., & Mowlavi, N. 2013, *MNRAS*, 434, 2238
- Anderson, R. I., Sahlmann, J., Holl, B., et al. 2015, *ApJ*, 804, 144
- Anderson, R. I., Saio, H., Ekström, S., Georgy, C., & Meynet, G. 2016a, *A&A*, 591, A8
- Anderson, R. I., Casertano, S., Riess, A. G., et al. 2016b, *ApJS*, 226, 18
- Astropy Collaboration, Robitaille, T. P., Tollerud, E. J., et al. 2013, *A&A*, 558, A33
- Baranowski, R., Smolec, R., Dimitrov, W., et al. 2009, *MNRAS*, 396, 2194
- Beaton, R. L., Freedman, W. L., Madore, B. F., et al. 2016, *ApJ*, 832, 210
- Benedict, G. F., McArthur, B. E., Feast, M. W., et al. 2007, *AJ*, 133, 1810
- Bhardwaj, A., Kanbur, S. M., Macri, L. M., et al. 2016, *MNRAS*, 457, 1644
- Bonvin, V., Courbin, F., Suyu, S. H., et al. 2017, *MNRAS*, 465, 4914
- Boutloukos, S. G., & Lamers, H. J. G. L. M. 2003, *MNRAS*, 338, 717
- Bresolin, F., Pietrzyński, G., Gieren, W., & Kudritzki, R.-P. 2005, *ApJ*, 634, 1020
- Cardelli, J. A., Clayton, G. C., & Mathis, J. S. 1989, *ApJ*, 345, 245
- Cardona, W., Kunz, M., & Pettorino, V. 2017, *JCAP*, 3, 056
- Casertano, S., Riess, A. G., Anderson, J., et al. 2016, *ApJ*, 825, 11
- Dalcanton, J. J., Williams, B. F., Lang, D., et al. 2012, *ApJS*, 200, 18
- de Grijs, R., Bastian, N., & Lamers, H. J. G. L. M. 2003, *MNRAS*, 340, 197
- Del Pozzo, W. 2012, *PhRvD*, 86, 043011
- Dhawan, S., Jha, S. W., & Leibundgut, B. 2017, ArXiv e-prints, arXiv:1707.00715
- Dias, W. S., Alessi, B. S., Moitinho, A., & Lépine, J. R. D. 2002, *A&A*, 389, 871
- Ekström, S., Georgy, C., Eggenberger, P., et al. 2012, *A&A*, 537, A146
- Evans, N. R., Bond, H. E., Schaefer, G. H., et al. 2016a, *AJ*, 151, 129
- Evans, N. R., Pillitteri, I., Wolk, S., et al. 2016b, *AJ*, 151, 108
- Follin, B., & Knox, L. 2017, ArXiv e-prints, arXiv:1707.01175
- Freedman, W. L., & Madore, B. F. 2010, *ARA&A*, 48, 673
- Freedman, W. L., Madore, B. F., Gibson, B. K., et al. 2001, *ApJ*, 553, 47
- Friel, E. D. 2013, *Open Clusters and Their Role in the Galaxy*, ed. T. D. Oswalt & G. Gilmore, 347
- Gaia Collaboration, Brown, A. G. A., Vallenari, A., & et al. 2016a, *A&A*, 595, A2
- Gaia Collaboration, Clementini, G., Eyer, L., & et al. 2017a, *A&A*, 605, A79
- Gaia Collaboration, Prusti, T., de Bruijne, J. H. J., & et al. 2016b, *A&A*, 595, A1
- . 2016c, *A&A*, 595, A1
- Gaia Collaboration, van Leeuwen, F., Vallenari, A., & et al. 2017b, *A&A*, 601, A19
- Gaia Collaboration, Eyer, L., Mowlavi, N., et al. 2017c, ArXiv e-prints, arXiv:1702.03295
- Gallenne, A., Mérand, A., Kervella, P., et al. 2015, *A&A*, 579, A68
- . 2016, *MNRAS*, 461, 1451
- García-Varela, A., Sabogal, B. E., & Ramírez-Tannus, M. C. 2013, *MNRAS*, 431, 2278
- Garmany, C. D., Conti, P. S., & Massey, P. 1980, *ApJ*, 242, 1063
- Georgy, C., Ekström, S., Granada, A., et al. 2013, *A&A*, 553, A24
- Gieren, W., Pilecki, B., Pietrzyński, G., et al. 2014, *ApJ*, 786, 80
- Goodwin, S. P., & Bastian, N. 2006, *MNRAS*, 373, 752
- Halbwachs, J.-L., Mayor, M., & Udry, S. 2017, *MNRAS*, 464, 4966
- Hoffmann, S. L., Macri, L. M., Riess, A. G., et al. 2016, *ApJ*, 830, 10
- Humphreys, E. M. L., Reid, M. J., Moran, J. M., Greenhill, L. J., & Argon, A. L. 2013, *ApJ*, 775, 13

- Inno, L., Matsunaga, N., Bono, G., et al. 2013, *ApJ*, 764, 84
- Johnson, L. C., Seth, A. C., Dalcanton, J. J., et al. 2015, *ApJ*, 802, 127
- . 2016, *ApJ*, 827, 33
- Kim, S., Staveley-Smith, L., Dopita, M. A., et al. 1998, *ApJ*, 503, 674
- Kodric, M., Riffeser, A., Hopp, U., et al. 2013, *AJ*, 145, 106
- Kodric, M., Riffeser, A., Seitz, S., et al. 2015, *ApJ*, 799, 144
- Lada, C. J., & Lada, E. A. 2003, *ARA&A*, 41, 57
- Leavitt, H. S., & Pickering, E. C. 1912, Harvard College Observatory Circular, 173, 1
- Livio, M., & Riess, A. G. 2013, *Physics Today*, 66, 41
- Madore, B. F. 1982, *ApJ*, 253, 575
- Manzotti, A., Dodelson, S., & Park, Y. 2016, *PhRvD*, 93, 063009
- Marigo, P., Girardi, L., Bressan, A., et al. 2017, *ApJ*, 835, 77
- McMillan, P. J. 2011, *MNRAS*, 414, 2446
- Mochejska, B. J., Macri, L. M., Sasselov, D. D., & Stanek, K. Z. 2000, *AJ*, 120, 810
- . 2001, *ArXiv Astrophysics e-prints*, astro-ph/0103440
- Moe, M., & Di Stefano, R. 2016, *ArXiv e-prints*, arXiv:1606.05347
- Moekel, N., Holland, C., Clarke, C. J., & Bonnell, I. A. 2012, *MNRAS*, 425, 450
- Musella, I., Marconi, M., Stetson, P. B., et al. 2016, *MNRAS*, 457, 3084
- Neilson, H. R., Schneider, F. R. N., Izzard, R. G., Evans, N. R., & Langer, N. 2015, *A&A*, 574, A2
- Ngeow, C., & Kanbur, S. M. 2006, *ApJ*, 650, 180
- Perlmutter, S., Aldering, G., Goldhaber, G., et al. 1999, *ApJ*, 517, 565
- Pietrzyński, G., & Udalski, A. 1999, *AcA*, 49, 543
- Pietrzyński, G., Thompson, I. B., Gieren, W., et al. 2010, *Nature*, 468, 542
- Planck Collaboration, Ade, P. A. R., Aghanim, N., & et al. 2016, *A&A*, 594, A13
- Riess, A. G., Casertano, S., Anderson, J., MacKenty, J., & Filippenko, A. V. 2014, *ApJ*, 785, 161
- Riess, A. G., Fliri, J., & Valls-Gabaud, D. 2012, *ApJ*, 745, 156
- Riess, A. G., Filippenko, A. V., Challis, P., et al. 1998, *AJ*, 116, 1009
- Riess, A. G., Macri, L., Casertano, S., et al. 2011, *ApJ*, 730, 119
- Riess, A. G., Macri, L. M., Hoffmann, S. L., et al. 2016, *ApJ*, 826, 56
- Sakai, S., Ferrarese, L., Kennicutt, Jr., R. C., & Saha, A. 2004, *ApJ*, 608, 42
- Sandage, A. 1958, *ApJ*, 128, 150
- Sandage, A., Tammann, G. A., & Reindl, B. 2004, *A&A*, 424, 43
- Senchyna, P., Johnson, L. C., Dalcanton, J. J., et al. 2015, *ApJ*, 813, 31
- Soszynski, I., Poleski, R., Udalski, A., et al. 2008, *AcA*, 58, 163
- Soszyński, I., Udalski, A., Szymański, M. K., et al. 2017, *ArXiv e-prints*, arXiv:1706.09452
- Stanek, K. Z., & Udalski, A. 1999, *ArXiv Astrophysics e-prints*, astro-ph/9909346
- Storm, J., Carney, B. W., Gieren, W. P., et al. 2004, *A&A*, 415, 531
- Suyu, S. H., Treu, T., Blandford, R. D., et al. 2012, *ArXiv e-prints*, arXiv:1202.4459, 1202.4459
- Szabados, L. 2003, in *Astronomical Society of the Pacific Conference Series*, Vol. 298, *GAIA Spectroscopy: Science and Technology*, ed. U. Munari, 237
- Tamm, A., Tempel, E., Tenjes, P., Tihhonova, O., & Tuvikene, T. 2012, *A&A*, 546, A4
- Tammann, G. A., & Reindl, B. 2002, *Ap&SS*, 280, 165
- Testa, V., Marconi, M., Musella, I., et al. 2007, *A&A*, 462, 599
- Udalski, A., Kubiak, M., & Szymanski, M. 1997, *AcA*, 47, 319
- Udalski, A., Soszynski, I., Szymanski, M., et al. 1999a, *AcA*, 49, 223
- . 1999b, *AcA*, 49, 437
- Vilardell, F., Jordi, C., & Ribas, I. 2007, *A&A*, 473, 847
- Wagner-Kaiser, R., Sarajedini, A., Dalcanton, J. J., Williams, B. F., & Dolphin, A. 2015, *MNRAS*, 451, 724
- Weinberg, D. H., Mortonson, M. J., Eisenstein, D. J., et al. 2013, *PhR*, 530, 87
- Welch, D. L., & Stetson, P. B. 1993, *AJ*, 105, 1813
- Wielgórski, P., Pietrzyński, G., Gieren, W., et al. 2017, *ApJ*, 842, 116
- Williams, B. F., Lang, D., Dalcanton, J. J., et al. 2014, *ApJS*, 215, 9
- Wolff, S. C. 1978, *ApJ*, 222, 556